

## RAPID COMMUNICATIONS

The purpose of this Rapid Communications section is to provide accelerated publication of important new results in the fields regularly covered by *Journal of Materials Research*. Rapid Communications cannot exceed four printed pages in length, including space allowed for title, figures, tables, references, and an abstract limited to about 100 words.

---

### Silicoaluminum carbonitride ceramic resist to oxidation/corrosion in water vapor

Yiguang Wang and Weifeng Fei

*Advanced Materials Processing and Analysis Center, University of Central Florida, Orlando, Florida 32816*

Yi Fan and Ligong Zhang

*Laboratory of Excited State Process, Changchun Institute of Optics, Fine Mechanics and Physics, Chinese Academy of Sciences, Changchun 130032, People's Republic of China*

Wenge Zhang

*Sporian Microsystem Inc., Lafayette, Colorado 80026*

Linan An<sup>a)</sup>

*Advanced Materials Processing and Analysis Center, University of Central Florida, Orlando, Florida 32816*

(Received 8 February 2006; accepted 16 April 2006)

The oxidation behavior of polymer-derived SiAlCN ceramic in a water vapor environment was studied at 1400 °C. The oxidation and corrosion rates of the SiAlCN are much lower than those of SiCN and pure silicon-based ceramics. The material retains about 75% of its original strength after exposure in water vapor for 300 h at 1400 °C. It is believed that the superior resistance of the SiAlCN to water vapor-related oxidation and corrosion is due to the formation of an aluminum-doped silica layer, in which the aluminum has reduced the activity of the silica.

Because of their excellent thermal and mechanical properties at elevated temperatures, covalent ceramics based on silicon carbide and nitride are under investigation for the fabrication of engine and turbine parts.<sup>1,2</sup> However, these important applications are limited by the fact that Si-based materials suffer severe degradation when exposed to high-temperature water vapor containing environments,<sup>3,4</sup> which exist when fossil fuel is converted to energy by combustion. The oxidation and corrosion of Si-based ceramics in water vapor occur through two distinct concurrent processes<sup>3</sup>: a reaction between silicon and water vapor to form a silicon dioxide scale (referred to as oxidation), and a reaction between the silica scale and water vapor to form volatile Si(OH)<sub>4</sub> (referred to as corrosion). The material degradation associated with the corrosion is twofold: (i) material recession, which reduces the dimensions of components, and (ii) surface defects, such as bubbles and cracks,<sup>5,6</sup> which

cause a marked decrease in mechanical strength.<sup>7</sup> Water vapor induced material degradation is a long-standing problem and is the most critical limiting factor for applications of Si-based ceramics.

In this communication, we describe a SiAlCN ceramic that has remarkably high resistance to water vapor related oxidation and corrosion at 1400 °C. We demonstrate that the oxidation and corrosion rates of the material are about an order of magnitude lower than the lowest values reported for silicon carbide and nitride. Furthermore, the material shows no corrosion-related surface defects, and more than 75% of its original strength is retained after long-term exposure to water vapor.

The polyaluminasilazane precursor used in this study was synthesized by dissolving 2 g aluminum isopropoxide powder (AlI; Alfa Aesar, Ward Hill, MA) into 8 g liquid-phased polyureamethylvinylsilazane (Ceraset, Kion, Huntingdon Valley, PA) by stirring for 1 h at room temperature. The mixture was then placed in a vacuum oven and heat-treated at 150 °C for 4 h. The resulting polyaluminasilazane was a viscous liquid with a pale yellow color. The fully dense ceramics were obtained using a pressure-assisted pyrolysis technique.<sup>8</sup> The liquid

<sup>a)</sup>Address all correspondence to this author.

e-mail: lan@mail.ucf.edu  
DOI: 10.1557/JMR.2006.0210

precursor was first solidified into a transparent solid by annealing at 150 °C for half an hour in ultrahigh-purity N<sub>2</sub> with the additive of 3 wt% dicumyl peroxide as an initiator. The solid was then cut into 12.5-mm-diameter disks that were 2–3 mm thick. The disks were pyrolyzed at 1400 °C for 6 h under 50 MPa isostatic pressure using ultrahigh-purity N<sub>2</sub> as the pressure media. The resultant ceramic disks were fully dense and about 10 mm in diameter and 1.5–2 mm thick. For comparison, fully dense SiCN disks were also prepared by the same procedure using pure Ceraset as the precursor. The compositions of the SiCN and SiAlCN ceramics were measured using elemental analysis and secondary hydrochloric acid inductively coupled plasma (ICP). The results are listed in Table I.

For the oxidation/corrosion tests, the ceramic disks with polished surfaces were annealed at 1400 °C in a mixture of 50% H<sub>2</sub>O–50% O<sub>2</sub>, flowing at a rate of 4.4 cm/s. The weight change of the samples was measured as a function of annealing time. The collective surface area of the samples was chosen to be over 15 cm<sup>2</sup> to ensure accuracy. The surface of the oxidized samples was observed using scanning electron microscopy (SEM; JEOL 6400F, Tokyo, Japan). The phases of the oxide scale were determined by x-ray diffraction (XRD; Rigaku, Tokyo, Japan).

For measuring the retained strength, testing bars 8 mm long and 1 × 2 mm in cross-section were cut from the disks and annealed under the same conditions as above. The strength of the annealed bars was then measured using a three-point bending method.

Figure 1 plots the weight change as a function of annealing time for the SiAlCN and SiCN. The oxidation and corrosion kinetic constants were obtained by fitting the experimental data with a parabolic kinetic model, which is expressed as<sup>4,9</sup>

$$t = \frac{\alpha^2 k_p}{2k_1^2} \left[ \frac{-2k_1 \Delta w_1}{\alpha k_p} - \ln \left( 1 - \frac{2k_1 \Delta w_1}{\alpha k_p} \right) \right],$$

$$\Delta w_2 = \beta k_1 t, \quad (1)$$

where  $k_p$  is the oxidation parabolic rate constant in the units of mg<sup>2</sup>/(cm<sup>4</sup>h),  $k_1$  is the linear rate constant in the units of mg/(cm<sup>2</sup>h),  $\Delta w_1$  is the weight gain due to the growth of SiO<sub>2</sub> scale,  $\Delta w_2$  is the weight loss due to

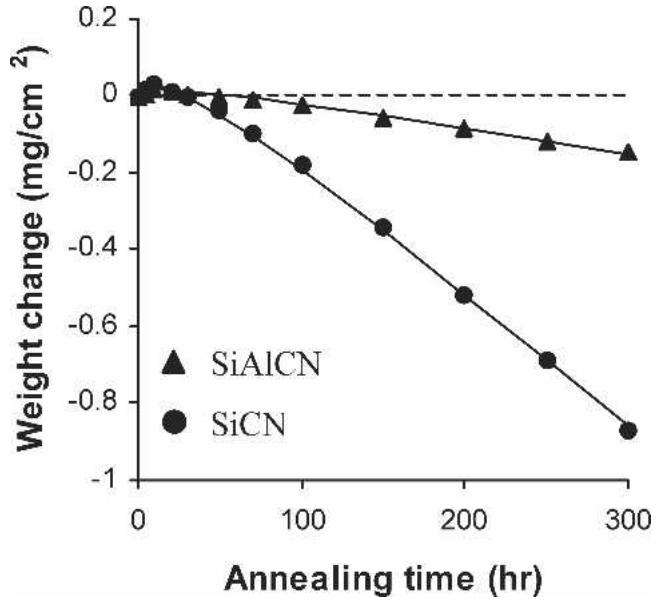


FIG. 1. Weight change of the samples as a function of oxidation time for the SiAlCN and SiCN. The data points are experimental results; the solid lines are theoretical fitting using Eqs. (1) and (2).

the volatilization of SiO<sub>2</sub>,  $t$  is the oxidation time, and  $\alpha$  and  $\beta$  are constants. For SiAl<sub>x</sub>C<sub>y</sub>N<sub>z</sub>O<sub>u</sub> ceramics,  $\alpha$  and  $\beta$  can be expressed as

$$\alpha = \frac{MW_{SiO_2} + \frac{x}{2} MW_{Al_2O_3}}{(1 + 3x/4 - u/2) MW_{O_2} - yMW_C - zMW_N},$$

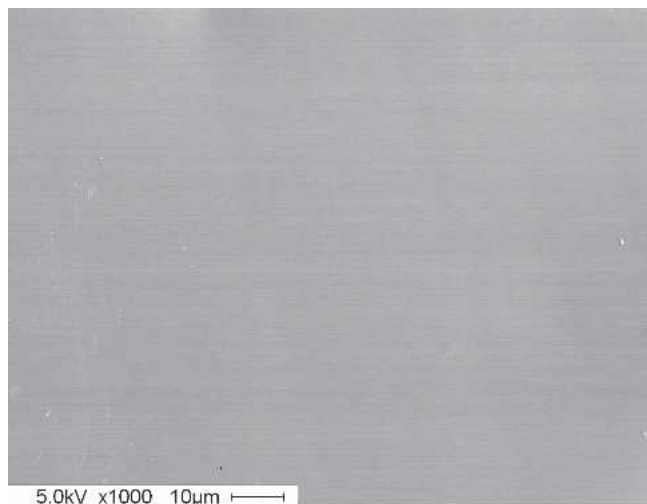
$$\beta = \frac{MW_{SiAl_xC_yN_z}}{MW_{SiO_2} + \frac{x}{2} MW_{Al_2O_3}}, \quad (2)$$

where  $MW$  is the molecular weight. The calculated  $k_1$  and  $k_p$  are listed in Table I, together with those for chemical vapor deposited (CVD) SiC and Si<sub>3</sub>N<sub>4</sub>. It can be seen that the  $k_1$  and  $k_p$  of the SiAlCN are, respectively, 5–7 and 10–80 times lower than those for the SiCN, CVD SiC, and Si<sub>3</sub>N<sub>4</sub>. These improvements are significant for water vapor related oxidation and corrosion. The corrosion rate of the SiAlCN is even lower than that of mullite, which is currently under development as an environmental barrier coating for protecting silicon carbide and nitride.<sup>10</sup>

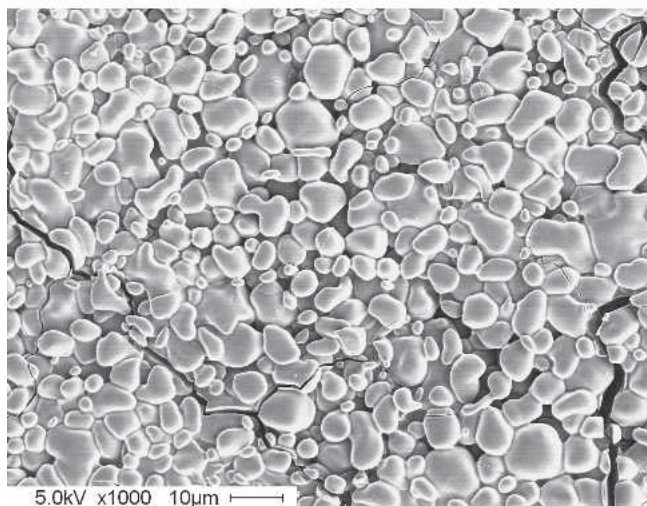
TABLE I. Materials and their oxidation and corrosion kinetic constants.

|  | SiAlCN   | SiCN  | CVD SiC <sup>4</sup> | CVD Si <sub>3</sub> N <sub>4</sub> <sup>6</sup> |
|--|--|---|----------------------|---|
| Precursor (Ceraset-to-Als weight ratio)                | 8:2  | 10:0  | ...                  | ...   |
| Compositions   | SiAl <sub>0.08</sub> C <sub>0.80</sub> N <sub>0.95</sub> O <sub>0.15</sub> | SiC <sub>0.99</sub> N <sub>0.85</sub> O <sub>0.11</sub> | ...                  | ...   |
| $k_1 \times 10^3$ (mg/cm <sup>2</sup> h)               | 0.98   | 4.9   | 6.4 <sup>a</sup>     | 6.2 <sup>a</sup>                                |
| $k_p \times 10^4$ (mg <sup>2</sup> /cm <sup>4</sup> h) | 0.53   | 4.9   | 39.3 <sup>a</sup>    | 10 <sup>a</sup>                                 |

<sup>a</sup> $k_1$  and  $k_p$  for CVD SiC and Si<sub>3</sub>N<sub>4</sub> were measured under the same conditions as those used in the present study.



(a)



(b)

FIG. 2. SEM images showing the surfaces of (a) SiAlCN and (b) SiCN after annealing for 300 h.

Figure 2 shows SEM images of the surfaces of the SiAlCN and SiCN after annealing for 300 h. The surface of the SiAlCN appears smooth and almost featureless [Fig. 2(a)]. In contrast, under the same annealing conditions, the surface of the SiCN (without aluminum-doping) was severely corroded to form river-bed-rock-like morphology and cracks [Fig. 2(b)] due to the volatilization of silica. The formation of corrosion-related defects, which are often observed for silicon carbide and nitride,<sup>3,6,7,11</sup> is one of the most predominant causes of material degradation.

Lack of surface defects allows the SiAlCN to exhibit excellent strength retention even after long-term annealing in water vapor environments (Fig. 3). The retained strength of the SiAlCN after annealing for 300 h is more than 75% of its original value, while the strength of the SiCN is reduced to only 20% of its original strength

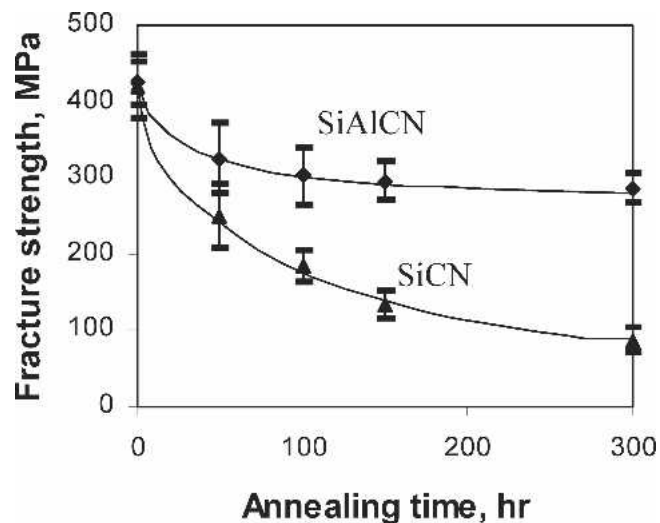


FIG. 3. Fracture strength of SiAlCN and SiCN as a function of annealing time.

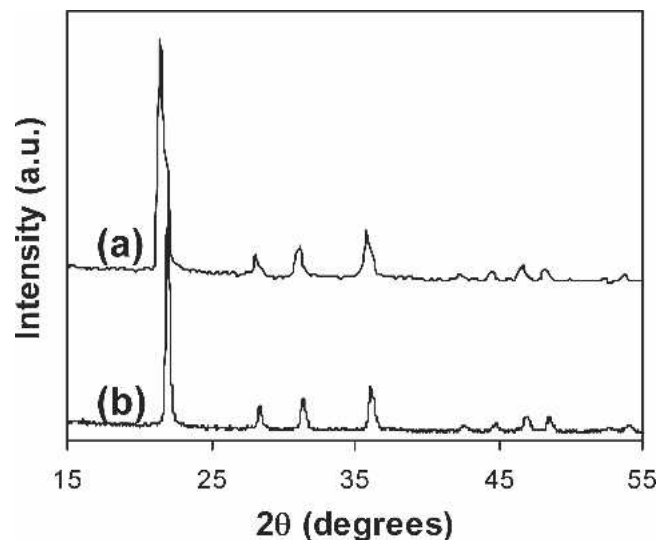


FIG. 4. X-ray diffraction patterns of (a) SiAlCN and (b) SiCN after annealing for 300 h.

under the same annealing conditions. It can also be noted from the figure that most of the reduction in the strength of the SiAlCN occurs in the first 100 h of annealing. Beyond 100 h, its strength remains nearly unchanged, suggesting that the material should have a long service life. The severe strength reduction due to water vapor corrosion was also observed in silicon carbide and nitride.<sup>7</sup>

To understand the enhanced resistance of the SiAlCN to water vapor related oxidation and corrosion, the oxide scales formed on the SiAlCN and SiCN are characterized. According to elemental analysis, the oxide scale formed on the SiCN is pure silica, and that formed on the SiAlCN is Al-containing silica. X-ray diffraction suggests that both oxides are pure cristobalite (Fig. 4). The

lattice parameters of the cristobalite phases are calculated using the XRD patterns: for the oxide formed on the SiCN,  $a = 0.4972$  nm and  $c = 0.6916$  nm, which are similar to the standard values for cristobalite (PDF card: 00-039-1425); for the oxide formed on the SiAlCN,  $a = 0.5019$  nm and  $c = 0.7426$  nm, which are much larger than the standard values for cristobalite, suggesting the formation of an  $\text{Al}_2\text{O}_3$ - $\text{SiO}_2$  solid solution. We believed that the Al doping in silica plays a key role in improving the resistance of the SiAlCN to water vapor related oxidation and corrosion.

The activity,  $a_{\text{SiO}_2(\text{Al}_2\text{O}_3-\text{SiO}_2)}$ , of  $\text{SiO}_2$  in the Al-doped silica layer can be estimated by comparison of the corrosion kinetic constant  $k_1$  of the SiAlCN and SiCN according to following equation:

$$\frac{a_{\text{SiO}_2(\text{Al}_2\text{O}_3-\text{SiO}_2)}}{a_{\text{SiO}_2}} = \frac{k_1(\text{SiAl}_{0.08}\text{C}_{0.80}\text{N}_{0.95}\text{O}_{0.15})}{k_1(\text{SiC}_{0.99}\text{N}_{0.85}\text{O}_{0.11})} \quad (3)$$

If the values of  $k_1$  for the SiAlCN and SiCN listed in Table I are inserted and the activity of pure silica,  $a_{\text{SiO}_2}$ , is assumed to be equal to unity (standard state), the  $a_{\text{SiO}_2(\text{Al}_2\text{O}_3-\text{SiO}_2)}$  can then be calculated as 0.2. This value is even lower than the activity of the silica in mullite (0.3–0.4).<sup>12</sup> A previous study,<sup>13</sup> which experimentally measured the silica activity, also revealed that the activity of silica in silica containing a small amount of  $\text{Al}_2\text{O}_3$  was lower than that of mullite, which is consistent with the current results.

In summary, by showing low oxidation and corrosion rates and high strength retention, we clearly demonstrated that compared to pure silicon-based ceramics, SiAlCN has a markedly higher resistance to water vapor related oxidation and corrosion. Although the origin of the enhanced oxidation/corrosion resistance is not fully understood, our results suggest that aluminum plays a key role in lowering the activity of silica. The new SiAlCN has great potential for applications in combustion systems, where the direct use of silicon carbide and nitride is limited. Furthermore, because it is synthesized via a polymeric precursor route, the material lends itself to making unique ceramic components such as micro-electromechanical systems, micro-sensors,<sup>8</sup> fibers,<sup>14</sup> and

ceramic-matrix composites<sup>15</sup> that can be operated in high-temperature corrosive environments.

## REFERENCES

1. F. Wakai, Y. Kodama, S. Sakaguchi, N. Murayama, K. Izaki, and K.A. Niihara: A superplastic covalent crystal composite. *Nature* **344**, 421 (1990).
2. R. Raj: Fundamental research in structural ceramics for service near 2000 °C. *J. Am. Ceram. Soc.* **76**, 2147 (1993).
3. E.J. Opila, R.C. Robinson, D.X. Fox, R.A. Wenglarz, and M.K. Ferber: Additive effects on  $\text{Si}_3\text{N}_4$  oxidation/volatilization in water vapor. *J. Am. Ceram. Soc.* **86**, 1262 (2003).
4. E.J. Opila and R.E. Hann: Paralineer oxidation of CVD SiC in water vapor. *J. Am. Ceram. Soc.* **80**, 197 (1997).
5. E.J. Opila: Variation of the oxidation rate of silicon carbide with water-vapor pressure. *J. Am. Ceram. Soc.* **82**, 625 (1999).
6. D.J. Fox, E.J. Opila, Q.N. Nguyen, D.L. Humphrey, and S.M. Lewton: Paralineer oxidation of silicon nitride in a water-vapor/oxygen environment. *J. Am. Ceram. Soc.* **86**, 1256 (2003).
7. H. Klemm: Corrosion of silicon nitride materials in gas turbine environment. *J. Eur. Ceram. Soc.* **22**, 2735 (2002).
8. L. Liew, W. Zhang, L. An, S. Shah, R. Lou, Y. Liu, T. Cross, K. Anseth, V. Bright, and R. Raj: Ceramic MEMS—new materials, innovative processing and futuristic applications. *Am. Ceram. Soc. Bull.* **80**, 25 (2001).
9. C.S. Tedmon: The effect of oxide volatilization on the oxidation kinetics of Cr and Cr-Fe alloys. *J. Electrochem. Soc.* **142**, 925 (1967).
10. K.N. Lee, D.S. Fox, J.I. Eldridge, D. Zhu, R.C. Robinson, N.P. Bansal, and R.A. Miller: Upper temperature limit of environmental barrier coatings based on mullite and BSAS. *J. Am. Ceram. Soc.* **86**, 1299 (2003).
11. P.F. Tortorelli and K.L. More: Effects of high water-vapor pressure on oxidation of silicon carbide at 1200 °C. *J. Am. Ceram. Soc.* **86**, 1249 (2003).
12. H. Mao, M. Selleby, and B. Sundman: Phase equilibria and thermodynamics in the  $\text{Al}_2\text{O}_3$ - $\text{SiO}_2$  system—modeling of mullite and liquid. *J. Am. Ceram. Soc.* **88**, 2544 (2005).
13. A. Dhima, B. Stafa, and M. Allibert: Activity measurement in steel-making-related oxides melts by differential mass spectrometry. *High Temp. Sci.* **21**, 143 (1986).
14. S. Yajima, Y. Hasegawa, K. Okamura, and T. Matsuzawa: Development of high-tensile-strength silicon carbide fiber using an organosilicon polymer precursor. *Nature* **273**, 525 (1978).
15. L. An, W. Xu, S. Rajagopalan, C. Wang, H. Wang, J. Kapat, L. Chow, Y. Fan, L. Zhang, D. Jiang, B. Guo, J. Liang, and R. Vaidyanathan: Carbon nanotube reinforced polymer-derived ceramic composites. *Adv. Mater.* **16**, 2036 (2004).